

Improvement of electronic focalization and consideration of material characteristics for numerical and experimental studies of phased array technique

B. Dupont, F. Zhang, H. Walaszek
French Industrial and Mechanical Technical Centre (CETIM)
Senlis (60300), France
benoit.dupont@cetim.fr

M. Ben Tahar
University of Technology of Compiègne (UTC), Laboratoire de Roberval
Compiègne (60200), France

Abstract

In CETIM, the French Industrial and Mechanical Technical Centre, the interest of modelling non destructive testing has to be shown. In our mission towards our contributors and customers, the proof of a good correlation between simulation and experimentations enables numerical studies instead of preliminary expensive experimental handlings.

This paper first presents performance of ultrasonic phased array technology and finally the correlation between simulated and experimental results. The influence of material characteristics for simulation is studied. Furthermore, a solution to improve electronic focusing is proposed in this paper.

1. Introduction

Ultrasonic phased array transducers are more and more used in the field of NDT industry. This PA technology offers well-known possibilities like electronic focalization and modelling is easy to associate with.

In order to obtain the best correlation between numerical results and experimental acquisitions, we can describe precisely the materials controlled. The parameters for simulation are determined experimentally. However, characterizing attenuation of material and structural noise can lead to fastidious and expensive handlings. In this paper, the interest of such a characterization of materials is studied.

Moreover, beam focalization obtained with time delay laws can be improved applying amplitude laws to the elements of a transducer. Thus it is possible to favour external elements of a transducer or on the contrary the internal elements. This paper presents the influence of apodisation of the ultrasonic beam on the defect response.

2. Conditions of study and material characterisation

2.1 Sample

The sample is made of 316L stainless steel. It is 80-mm thick. The sample contains flat bottom holes of different diameters and depths, described below.

Table 1. Holes drilled in stainless steel sample

Diameter (mm), Constant depth: 10 mm	0.3	0.5	0.8	1	2
Depth (mm), Constant diameter: 1 mm	20	40	60	70	75

For the numerical study, in order to obtain results as real as possible, material properties are determined. Thus, wave velocity is measured experimentally. Longitudinal wave velocity is $5700 \text{ m}\cdot\text{s}^{-1}$. Material attenuation and structural noise are now characterised thanks to experimentation.

2.1.1 Attenuation of ultrasound

Attenuation in materials is mainly due to diffusion at grain boundaries. The attenuation of ultrasound in material is determined thanks to the method described in Figure 1. Two identical transducers are used immersed in water: the first one in transmission, the second one in reception, exactly facing the first. The principle consists in recording two signals in transmission. The first one is acquired through water and provides the reference signal $r(t)$. The second one $s(t)$ through the sample inserted between the transducers.⁽¹⁾

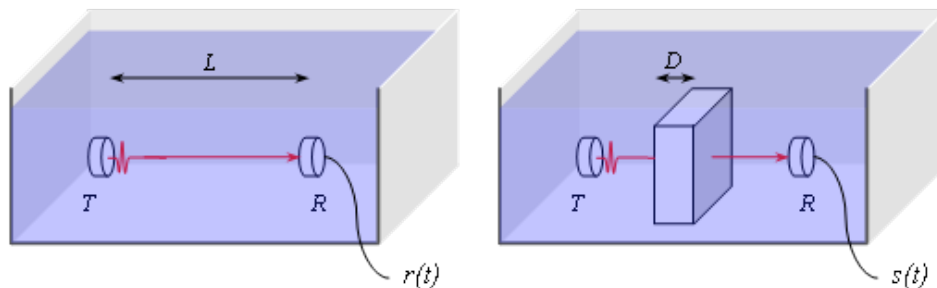


Figure 1. Experimental setup

Given that the coefficient of attenuation $\alpha(f)$ is a function of frequency, the operation is repeated with different transducers of different frequencies. The coefficient is obtained computing the Fourier transform $R(f)$ and $S(f)$ of the two previous temporal signals and applying this formula:

$$\alpha(f) = \frac{1}{D} \left(\ln T - \ln \left| \frac{S(f)}{R(f)} \right| \right) + \alpha_{water} \dots \dots \dots (1)$$

Where D is the thickness of the sample, α_{water} the attenuation in water and T the transmission coefficient:

$$T = \frac{4\rho_{water}c_{water}\rho c}{(\rho_{water}c_{water} + \rho c)^2} \dots\dots\dots (2)$$

Attenuation, which is frequency-dependant, is defined in CIVA by a polynomial law.

$$\alpha(f) = \sum_{p=1}^n \alpha_p f^p \dots\dots\dots (3)$$

Where p is the power of frequency, f the frequency, and α_p the coefficient of the exponential monomial p . The attenuation curve obtained for the material is shown on Figure 2.

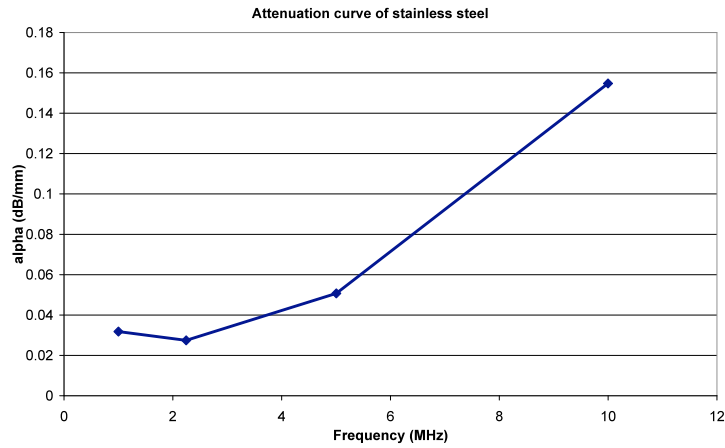


Figure 2. Polynomial attenuation curve for stainless steel

At high frequencies, material is more attenuating than at low frequencies. For example, at 2 MHz, the material has an attenuation of about 25 dB/m.

The values of α_p coefficients are then input into CIVA to define material attenuation.

2.1.2 Structural noise

As attenuation coefficient, parameters defining the structural noise have to be determined experimentally.

Structural noise is modelled in CIVA as a set of diffracting points randomly positioned in a part according to a uniform distribution scheme. The density of these points, i.e. the number of them per volume unit is determined by the parameter ρ .

A reflectivity amplitude is assigned at each diffracting point. It is determined randomly on the basis of a zero-mean Gaussian distribution and a standard deviation of σ .⁽²⁾

These two parameters are determined comparing a numerical signal to an experimental signal acquired in the part.

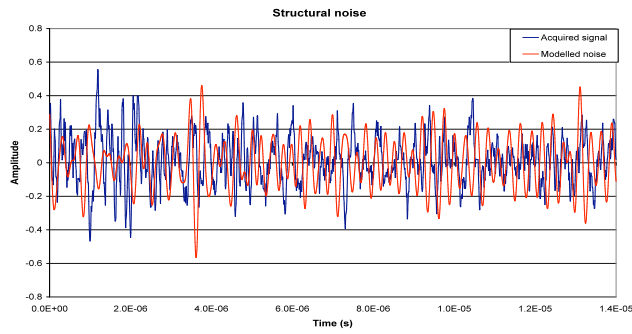


Figure 3. Comparison between modelled noise and acquired noise

2.2 Tools

The numerical study is made with the NDT simulation software CIVA developed by the French Atomic Energy Commission (CEA). Experimentations are lead on electronic-software Multi-X device distributed by M2M. Thus, the same interface for simulation and experimentations is used. Comparison between numerical and experimental results is possible. A 64-element linear array transducer of 2.25 MHz central frequency is used.

3. Numerical study

3.1 Beam computation

3.1.1 Amplitude laws

The influence of amplitude laws is studied. The following figure describes the different amplitude laws applied. A Uniform amplitude law consists in exciting every element with the same amplitude. A Hanning amplitude law excites central elements with higher amplitude than the external ones. In opposite, the external elements are excited with higher amplitude if Inverse Hanning amplitude law is used.

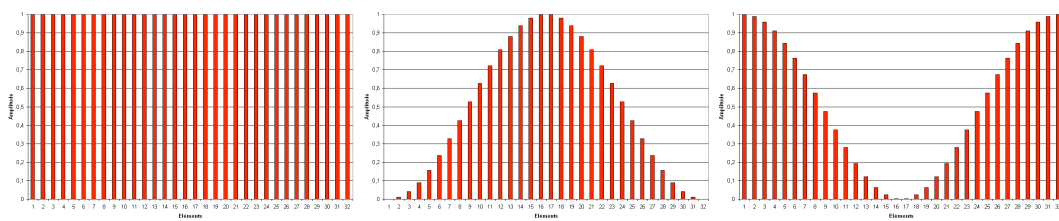


Figure 4. Amplitude laws: Uniform, Hanning, Inverse Hanning

Compared with Uniform amplitude excitation, a Hanning amplitude law reduces the aperture of the transducer. It increases focal length and width and gives a beam more homogeneous in the depth. This amplitude law is useful for detection.

On the other hand, an Inverse Hanning amplitude law reduces the focal width and increases the focal length. The near field zone is perturbed. This amplitude law can be used for sizing defects.

The holes drilled in the sample have different depths. To control all the thickness of the piece, the time delay laws applied allow beam focalization at several successive depths. The following figure shows the sum of the different beams obtained for time delay laws and the effect of the amplitude laws applied: Uniform, Hanning and Inverse Hanning. The beam is a convolution of the two transmission and reception fields.

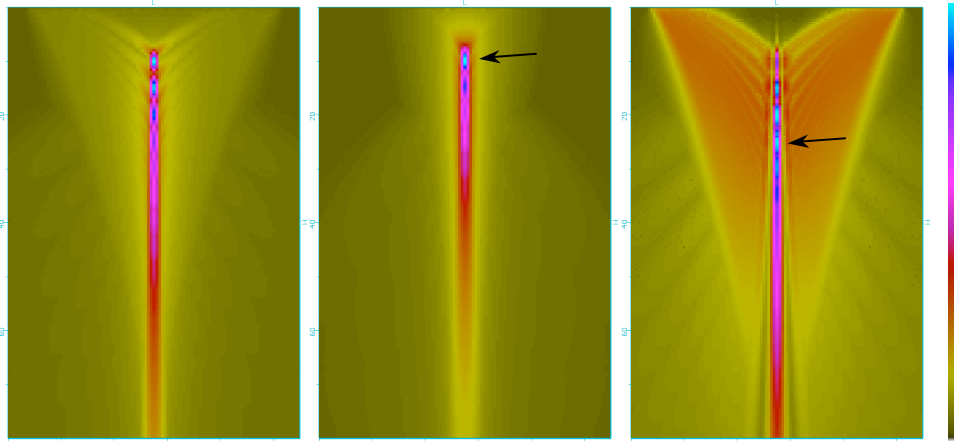


Figure 5. Influence of the amplitude laws on the beam: Uniform, Hanning, Inverse Hanning (summed field of the successive time delay laws applied)

As explained previously, the Figure 5 shows the homogeneous beam due to a Hanning amplitude law applied to the transducer. Moreover, the maximum of energy is near the surface for the first delay law (see arrow on figure) and decreases for the next laws.

The beam resulting from the Inverse Hanning amplitude law is effectively less wide and longer than for the other amplitude laws. The maximum of energy is obtained for the fourth delay law (arrow on figure) and decreases slowly for the next laws, compared with others. Moreover, the field is disrupted on the sides of the focal line.

The effect of amplitude law is now shown for one time delay law. The following figure presents the field for the eighth focal law calculated to focus the beam at 45 mm depth.

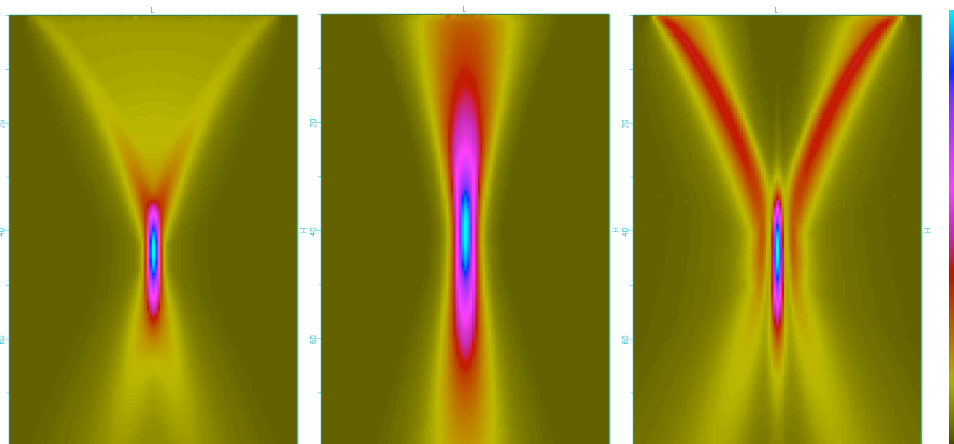


Figure 6. Beam focalization at 45 mm depth with Uniform, Hanning and Inverse Hanning amplitude laws

The beam is effectively homogeneous in depth for Hanning amplitude law. It is also less wide and longer for Inverse Hanning amplitude law, as seen in Table 2. The field is disrupted before and after the focal zone.

Table 2. Characteristics of the focal zone for different amplitude laws

Amplitude law	Focal point position (mm)	Focal length at -6 dB (mm)	Focal width at -6 dB (mm)
Uniform	43.5	18.1	2.3
Hanning	40.0	38.2	4.0
Inverse Hanning	43.5	20.1	1.8

3.1.2. Improvement of beam focalization

As explained in 3.1.1, each amplitude law has its advantages and disadvantages. The idea is here to take all these advantages to eliminate or reduce the disadvantages. Thus, the beam could be both homogeneous in depth and with a thin and long focal zone. That is possible applying an Inverse Hanning amplitude law for the transmission and a Hanning amplitude law for the reception.

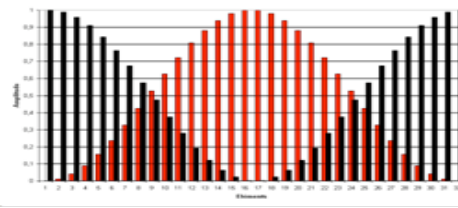


Figure 7. Combined amplitude law: Inverse Hanning (black, transmission) and Hanning (red, reception)

This combination gives the following beam (Figure 8), resulting from a convolution of the transmission (Inverse Hanning) and reception (Hanning) fields. It represents the sum of the different beams obtained for the successive time delay laws applied with this combined amplitude law.

Furthermore, to compare with other amplitude laws, the beam obtained for the eighth time delay law with this combined amplitude law is shown.

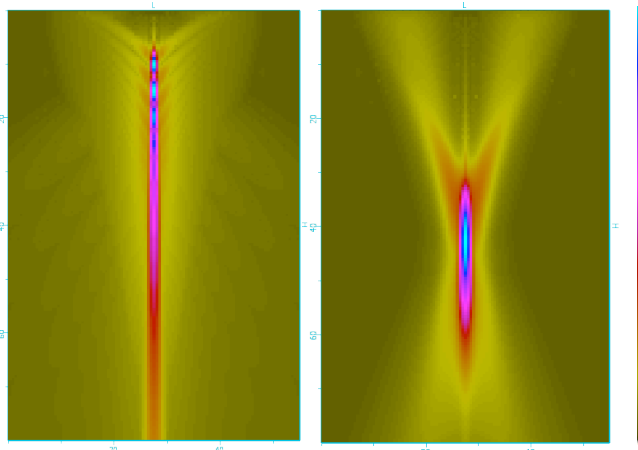


Figure 8. Combined amplitude law: summed field and beam focalization at 45 mm depth

Table 3. Characteristics of the focal zone for combined amplitude law

Amplitude law	Focal point position (mm)	Focal length at -6 dB (mm)	Focal width at -6 dB (mm)
Combined Inverse Hanning / Hanning	42.5	23.6	2.2

Comparing Table 2 and Table 3, the combined amplitude law gives a focal length longer than Uniform and Inverse Hanning laws but shorter than Hanning law. The focal width is smaller than Uniform and Hanning laws but slightly larger than Inverse Hanning law. Moreover, the beam is not as disrupted as for Inverse Hanning.

3.1.3 Attenuation

For beam computation, attenuation coefficient determined in part 2.1.1 reduces the amplitude of beam calculated without attenuation. Whatever amplitude law applied, at given depth, the attenuation of the beam is the same.

Table 4. Decrease of the amplitude when considering attenuation

Depth (mm)	Attenuation (dB)
10	- 0.6
45	- 2.7
80	- 4.5

An attenuation of - 4.5 dB for 80-mm depth is coherent with the value of attenuation given previously. Indeed, 80-mm depth represents an ultrasonic path of 160 mm for the wave. The value of attenuation is 28 dB/m.

3.2 Defect response

The reference for amplitude is the backwall echo measured without defect. The signal to noise ratio measured for reference is 64 dB. The influence of attenuation is also studied.

3.2.1 Variation of the holes diameter

The holes are 70-mm depth with diameters from 0.3 to 2 mm. The amplitudes of echoes are measured for each amplitude law. Numerical results are given in Figure 9.

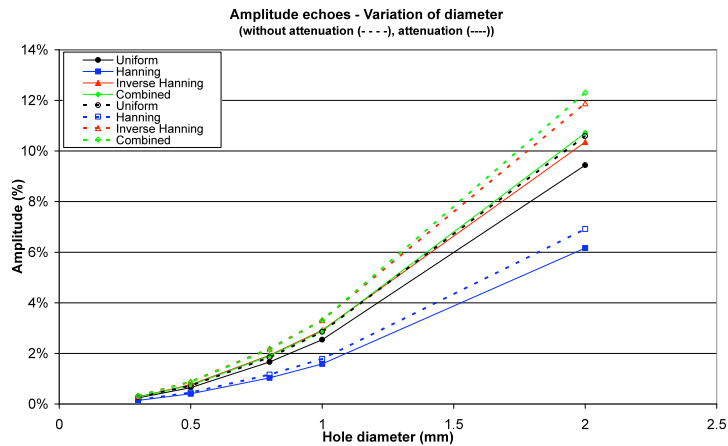


Figure 9. Modelled amplitude echoes for different diameter holes with attenuation or not

With the same reference for all the amplitude laws, numerical results give echoes of lower amplitude when Hanning amplitude law is applied. Results are close for Inverse Hanning and Combined amplitude laws, but the second one is slightly better.

3.2.2 Variation of the holes depth

Figure 10 shows the results for holes of 1-mm diameter and depths varying from 20 to 75 mm.

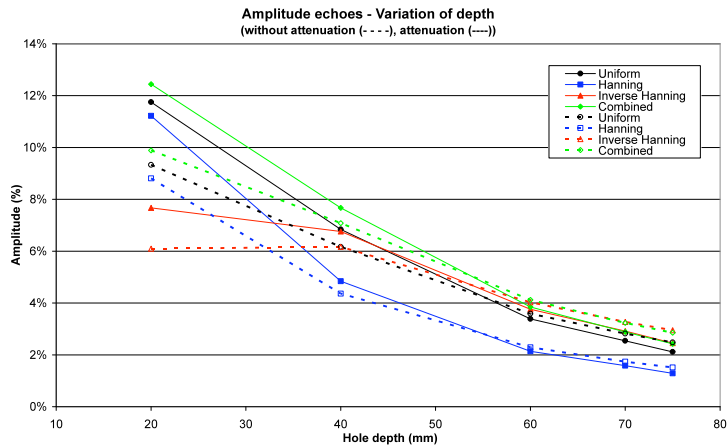


Figure 10. Modelled amplitude echoes for different depth holes with attenuation or not

As seen with beam computation, Inverse Hanning law does not give good result for not very deep hole. It is due to the disrupted beam between the surface and the focal zone. In opposite, Uniform, Hanning and Combined amplitude laws follow the same fall when defects are deeper. Compared with others, the Combined amplitude law still gives echoes of higher amplitude.

3.2.3 Attenuation and structural noise

The influence of attenuation for defect response calculation is shown on Figure 9 and Figure 10. Whatever amplitude law, for given diameter and depth, considering attenuation modifies the amplitude echo in the same proportions.

Furthermore, at low depths, amplitude echoes with attenuation are 20 % higher than without attenuation. For the moment, there is no explanation concerning this result. However, for defects of more than 40-mm depths, amplitude echoes without attenuation are higher than with attenuation, which is more logical.

Compared with measures without attenuation, for given diameter, the more deep is the hole, the more the echo is attenuated when attenuation is considered. Moreover, for constant depth, when diameter increases, the echo is slightly more attenuated when considering attenuation.

The modelled noise amplitude is very low. 64 dB correspond to a noise of 0.05 % of the reference amplitude.

3.3 Conclusion on numerical study

The value of attenuation determined experimentally and implemented in CIVA gives coherent results. For depths higher than 40 mm, signal with attenuation is effectively lower than signal without attenuation. The parameters describing structural noise seem to give low amplitude for the noise.

According to this numerical study, combining amplitude laws gives interesting results. The Inverse Hanning amplitude law is important to improve focal zone. The Hanning amplitude law homogenizes the beam. Combining the first for transmission and the last for reception improves results. Indeed, compared with Uniform amplitude law, the gains of the other amplitude laws are noted in Table 5.

Table 5. Gains of amplitude laws compared with Uniform law

Amplitude law	No attenuation	With attenuation
Hanning	- 3.9 dB	- 4.0 dB
Inverse Hanning	+ 1.2 dB	+ 1.0 dB
Combined	+ 1.3 dB	+ 1.1 dB

To conclude, attenuation does not change results for a given amplitude law applied. Moreover, the combined amplitude law studied improves results compared with Uniform law and gives better results than others.

4. Experimentations

In order to validate numerical study, experimentations are done applying the configurations modelled previously. The reference for amplitude is the backwall echo measured without defect. The signal to noise ratio measured for reference is 44 dB. It corresponds to 0.55 % of the reference amplitude, whatever amplitude laws.

4.1 Variation of the holes diameter

Like in numerical study, the holes are 70-mm depth. Diameters vary from 0.3 to 2 mm.

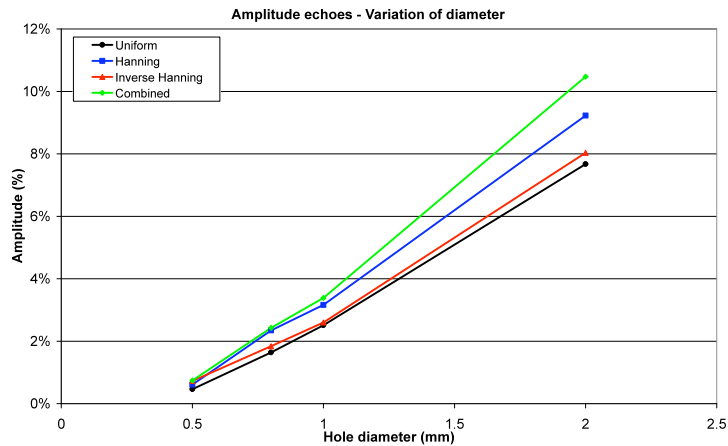


Figure 11. Experimental amplitude echoes of holes with different diameters

The echoes amplitude increases with the diameter. 0.3-mm diameter hole is not detected experimentally. The combined amplitude law gives the highest amplitude compared to other amplitude laws.

4.2 Variation of the holes depth

The holes diameter is 1 mm. Depths vary from 20 to 75 mm.

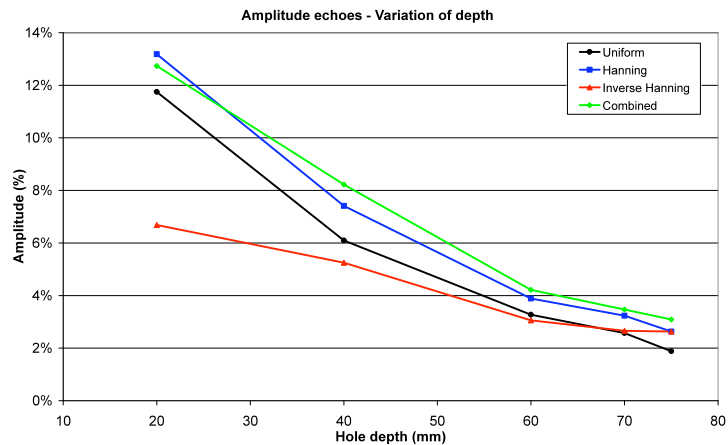


Figure 12. Experimental amplitude echoes of holes of different depths

The echoes amplitude decreases with depth. For very low depths, Inverse Hanning law does not give good amplitude compared with Uniform law. Combined amplitude law gives higher amplitudes than other configurations (Table 6).

Table 6. Experimental gains of amplitude laws compared with Uniform law

Amplitude law	Experimentation
Hanning	+ 2.1 dB
Inverse Hanning	+ 0.8 dB
Combined	+ 3.0 dB

5. Validation

In order to conclude on the interest of characterizing attenuation and structural noise, it is necessary to compare experimentations with numerical results. According to the numerical study, the combined amplitude law improves results. Experimentally, the combined amplitude law gives also better results. Thus, only the numerical results obtained with this amplitude law (with attenuation or not) will be compared with experimental results.

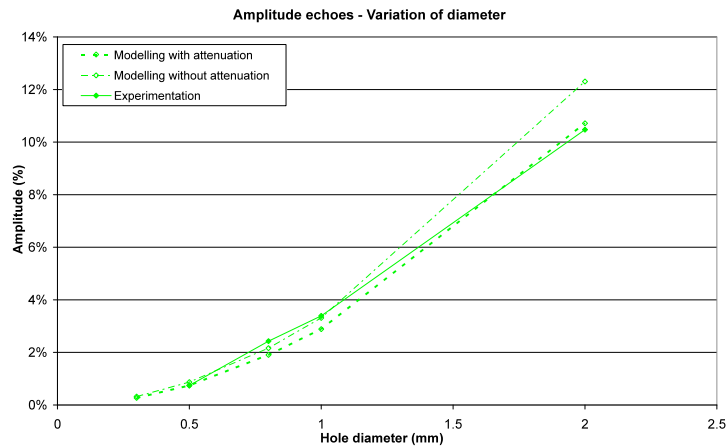


Figure 13. Comparison between experimental and numerical results, variation of diameter

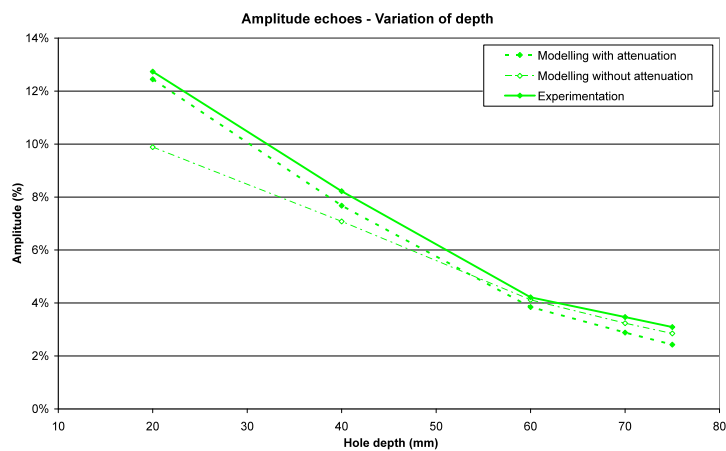


Figure 14. Comparison between experimental and numerical results, variation of depth

For a given depth with variation of diameter, numerical results obtained with attenuation are close to experimental results and a little under-estimated. The difference between modelling and experimentation is lower than 10 %.

For a given diameter with variation of depth, correlation between modelling and experimentation is good, especially if numerical results are obtained with attenuation. Calculation made without attenuation gives better results for the deepest holes. The difference between modelling and experimentation is about 11 %.

Numerical results obtained without attenuation are good compared with experimental results for small diameters and high depths. Those obtained with attenuation are good whatever diameters and depths.

Finally, the modelled structural noise does not prevent from detecting the smallest diameter hole. Experimentally, there was no detectable echo for this hole. The modelled noise is too weak compared to the real structural noise. However, to characterize noise in CIVA, it is necessary to know the real structural noise. Given that correlation between experimental and numerical results is good, it is possible to predict the echoes which will not be detected. Indeed, 0.3-mm diameter gives an echo of 0.27 % of reference and experimental structural noise is 0.55 %. This hole is obviously not detectable.

6. Conclusion

Ultrasonic phased array transducers allow electronic focusing when time delay laws are applied. It is possible to improve this focalization applying at the same time amplitude laws. Combining Inverse Hanning and Hanning amplitude laws improves much more this focalization, taking the advantages of each law and reducing their disadvantages.

Furthermore, the good correlation between numerical and experimental results is shown. However, it is quite absolutely necessary to properly characterize at least attenuation of ultrasound in material to determine performance and predict results thanks to simulation.

Reference

1. M.A. PLOIX, P. GUY, R. EL GOURJOUA, J. MOYSAN, G. CORNELOUP, B. CHASSIGNOLE, 'Attenuation assessment for NDT of austenitic stainless steel welds', ECNDT 2006.
2. S. CHATILLON, C. POIDEVIN, N. GENGEMBRE, A. LHEMERY, 'Simplified modelling of backscattered noise and attenuation phenomena for quantitative performance demonstration of UT methods', Review of Progress in QNDE 22, ed. by D. O. Thompson and D. E. Chimenti (AIP Conference Proceedings 657, Melville, 2003), pp. 93-100